

Soft Limits of Multiparticle Observables and Parton Hadron Duality ^{*}

Wolfgang Ochs

Max-Planck-Institut für Physik (Werner Heisenberg-Institut), Föhringer Ring 6,
D-80805 München, Germany

Abstract. We discuss observables in multiparticle production for three kinds of limits of decreasing kinematical scales: 1. the transition jet \rightarrow hadron (limit $y_{cut} \rightarrow 0$ of the resolution parameter y_{cut}); 2. single particle inclusive distributions normalized at threshold $\sqrt{s} \rightarrow 0$ and 3. particle densities in the limit of low momentum $p, p_T \rightarrow 0$. The observables show a smooth behaviour in these limits and follow the perturbative QCD predictions, originally designed for large scales, whereby a simple prescription is supplemented to take into account mass effects. A corresponding physical picture is described.

1 Introduction

A successful description of multiparticle production based on perturbative QCD has been established for "hard" processes which are initiated by an interaction of elementary quanta (quarks, leptons, gauge bosons, ...) at large momentum transfers $Q^2 \gg \Lambda^2$, whereby the characteristic scale in QCD is $\Lambda \sim \text{few } 100 \text{ MeV}$. In this kinematic regime the running coupling constant $\alpha_s(Q^2)$ is small and the lowest order terms of the perturbative expansion provide the desired accuracy. The coloured quarks and gluons which emerge from the primary hard process cannot escape towards large distances because of the confinement of the colour fields. Rather, they "fragment" into particle jets which may consist of many stable and unstable hadrons.

Here we are interested in the emergence of the hadronic final states and jet structure. The partons participating in the hard process generate parton cascades through gluon Bremsstrahlung and quark antiquark pair production processes which can be treated again perturbatively, at least approximately. The singular behaviour of the gluon Bremsstrahlung in the angle Θ and momentum k

$$\frac{dn}{dkd\Theta} \propto \alpha_s(k_T/\Lambda) \frac{1}{k\Theta}, \quad k_T > Q_0. \quad (1)$$

(in lowest order and for small angles) leads to the collimation of the partons and the jet structure. The transverse momentum k_T is taken as characteristic scale for the coupling $\alpha_s \sim 1/\ln(k_T/\Lambda)$, so it will rise with decreasing scale during jet evolution and one expects the perturbation theory to loose its validity below a limiting scale Q_0 .

The transition to the hadronic final state, finally, proceeds at small momentum transfers $k_T \sim Q_0$ by non-perturbative processes. There have been different approaches to obtain predictions on the hadronic final states:

^{*} Presented at Ringberg Workshop "New trends in HERA physics 1999", Tegernsee, Germany, May 30 - June 4, 1999

1. “Microscopic” Monte Carlo models

In a first step a parton final state is generated perturbatively corresponding to a cut-off scale like the above Q_0 . Then, according to a non-perturbative model intermediate hadronic systems (clusters, strings, ...) are formed which decay, partly through intermediate resonances, into the final hadrons of any flavour composition. Depending on the considered complexity a larger number of adjustable parameters are allowed for in addition to the QCD scale and cut-off parameters. Because of the complexity of these models only Monte Carlo methods are available for their analysis. They are able to reproduce many very detailed properties of the final state successfully.

2. Parton Hadron Duality approaches

One compares the perturbative QCD result for particular observables directly with the corresponding result for hadrons. The idea is that the effects of hadronization are averaged out for sufficiently inclusive observables. In this case analytical results are aimed for which are closer to a direct physical interpretation than the MC results (for reviews, see [1,2]). This general idea comes in various realizations, we emphasize three kinds of observables:

Jet cross sections: Jets are defined with respect to a certain resolution criterion (parameter y_{cut}), then the cross sections for hadron and parton jets are compared directly at the same resolution. This phenomenological ansatz has turned out to be extremely successful in the physics of energetic jets. A priori, it is non-trivial that an energetic hadron jet with dozens of hadrons should be compared directly to a parton jet with only very few (1-3) partons.

Infrared and collinear safe observables: The value of such an observable is not changed if a soft particle with $k \rightarrow 0$ or a collinear particle ($\Theta \rightarrow 0$) is added to the final state. It is then expected that the observables are less sensitive to the kinematic region $k_T \sim Q_0$ in (1). Especially, event shape observables like “Thrust” or energy flow patterns belong into this category. Perturbative calculations with all order resummations have been generally successful. In recent years perturbative calculations to $O(\alpha_s^2)$ in combination with power corrections $\sim 1/Q^q$ have found considerable interest.

Infrared sensitive observables: Global particle multiplicities as well as inclusive particle distributions and correlations belong into this category; these observables are divergent for $Q_0 \rightarrow 0$ and therefore are particularly sensitive to the transition region from partons to hadrons. Q_0 plays the role of a nonperturbative hadronization parameter.

In this report we will be concerned with the last class of observables to learn about the soft phenomena and ultimately about the colour confinement mechanisms. Specific questions concerning the role of perturbative QCD are

- What is the limiting value of Q_0 for which perturbative QCD can be applied successfully. Especially, can Q_0 be of the order of $\Lambda \sim \text{few } 100 \text{ MeV}$?
- Is there any evidence for the strong rise of the coupling constant α_s towards small scales below 1 GeV?
- Is there evidence for characteristic QCD coherence effects at small scales which are expected for soft gluons, evidence for the colour factors C_A, C_F ?

2 Theoretical approach

2.1 Partons

The evolution of a parton jet is described in terms of a multiparticle generating functional $Z_A(P, \Theta; \{u(k)\})$ with momentum test functions $u(k)$ for a primary parton A ($A = q, g$) of momentum P and jet opening angle Θ . This functional fulfils a differential-integral equation [1]

$$\begin{aligned} \frac{d}{d \ln \Theta} Z_A(P, \Theta) &= \frac{1}{2} \sum_{B,C} \int_0^1 dz \\ &\times \frac{\alpha_s(k_T)}{2\pi} \Phi_A^{BC}(z) [Z_B(zP, \Theta) Z_C((1-z)P, \Theta) - Z_A(P, \Theta)] \end{aligned} \quad (2)$$

and has to be solved with constraints $k_T > Q_0$ and with initial condition

$$Z_A(P, \Theta; \{u\})|_{P\Theta=Q_0} = u_A(k=P). \quad (3)$$

which means that at threshold $P\Theta = Q_0$ there is only one particle in the jet. From the functional Z_A one can obtain the inclusive n-parton momentum distributions by functional differentiation after the functions $u(k_i)$, $i = 1 \dots n$, at $u=1$ and then one finds the corresponding evolution equations as in (2). This “Master Equation” includes the following features: the splitting functions $\Phi_A^{BC}(z)$ of partons $A \rightarrow BC$; evolution in angle Θ yielding a sequential angular ordering which limits the phase space of soft emission as a consequence of colour coherence; the running coupling $\alpha_s(k_T)$. For large momentum fractions z the equation approaches the usual DGLAP evolution equations.

The solution of the evolution equations can be found by iteration and then generates an all order perturbation series; it is complete in leading order (“Double Logarithmic Approximation – DLA”) and in the next to leading order (“Modified Leading Log Approximation” – MLLA), i.e. in the terms $\alpha_s^n \log^{2n}(y)$ and $\alpha_s^n \log^{2n-1}(y)$. The logarithmic terms of lower order are not complete, but it makes sense to include them as well as they are important for taking into account energy conservation and the correct behaviour near threshold (3). The complete partonic final state of a reaction may be constructed by matching with an exact matrix element result for the primary hard process.

2.2 Hadrons

We investigate here the possibility that the parton cascade resembles the hadronic final state for sufficiently inclusive quantities. One motivation is “preconfinement” [3], the preparation of colour neutral clusters of limited mass within the perturbative cascade. If the cascade is evolved towards a low scale $Q_0 \sim \Lambda$, a successful description of inclusive single particle distributions has been obtained (“Local Parton Hadron Duality”-LPHD [4]). More generally, one could test relations between parton and hadron observables of the type

$$O(x_1, x_2, \dots)|_{\text{hadrons}} = K O(x_1, x_2, \dots; Q_0, \Lambda)|_{\text{partons}} \quad (4)$$

where the nonperturbative cut-off Q_0 and an arbitrary factor K are to be determined by experiment (for review, see [2]). In comparing differential parton and hadron distributions there can be a mismatch near the soft limit because of mass effects, especially, the (massless) partons are restricted by $k_T > Q_0$ in (2) but hadrons are not. This mismatch can be avoided by an appropriate choice of energy and momentum variables. In a simple model [5,6] one compares partons and hadrons at the same energy (or transverse mass) using an effective mass Q_0 for the hadrons, i.e.

$$E_{T,parton} = k_{T,parton} \quad \Leftrightarrow \quad E_{T,hadron} = \sqrt{k_{T,hadron}^2 + Q_0^2}, \quad (5)$$

then, the corresponding lower limits are $k_{T,parton} \rightarrow Q_0$ and $k_{T,hadron} \rightarrow 0$.

3 From Jets to Hadrons, the limit $y_{cut} \rightarrow 0$

We turn now to the discussion of several observables and their behaviour in the limit of a small scale. First, we consider the transition from jets to hadrons by decreasing the resolution scale of jets. Jet physics is a standard testing ground for perturbative QCD, the transition to hadrons therefore corresponds to the transition from the known to the unknown territory.

The jets are defined in the multiparticle final state by a cluster-algorithm. Popular is the ‘‘Durham algorithm’’ [8] which allows the all order summation in the perturbative analysis. For a given resolution parameter $y_{cut} = (Q_{cut}/Q)^2$ in a final state with total energy Q particles are successively combined into clusters until all relative transverse momenta are above the resolution parameter $y_{ij} = k_T^2/Q^2 > y_{cut}$.¹ We study now the mean jet multiplicity N_{jet} in the event as function of y_{cut} . In e^+e^- -annihilation for $y_{cut} \rightarrow 1$ all particles are combined into two jets and therefore $N_{jet} = 2$, on the other hand, for $y_{cut} \rightarrow 0$ all hadrons are resolved and $N_{jet} \rightarrow N_{had}$.

Results on jet multiplicities are shown in Fig. 1. The jet multiplicity rises only slowly with decreasing y_{cut} . For $y_{cut} \gtrsim 0.01$ the data are well described by the complete matrix element calculations to $O(\alpha_s^2)$ (first results of this kind in [9]) and allow the precise determination of the coupling or, equivalently, of the QCD scale parameter $\Lambda_{\overline{MS}}$ [10,11]. In the region above $y_{cut} > 10^{-3}$ the resummation of the higher orders in α_s becomes important [12] and the MLLA calculation describes the data well. The lower curve shown in Fig. 1 is obtained [7] from a full (numerical) solution of the evolution equations corresponding to (2), matched with the $O(\alpha_s)$ matrix element, and describes the data obtained at LEP-1 [10,11] down to 10^{-4} .

The theoretical curve diverges for small cut-off $Q_{cut} \rightarrow \Lambda$ as in this case the coupling $\alpha_s(k_T)$ diverges. In the duality picture discussed above the parton final state corresponds to a hadron final state at the resolution $k_T \sim Q_0$ according to (4) and this limit is reached for $Q_{cut} \rightarrow Q_0$. The calculation meets the hadron

¹ more precisely, the distance is defined by $y_{ij} = 2(1 - \cos \Theta_{ij}) \min(E_i^2 E_j^2)/Q^2 > y_{cut}$.

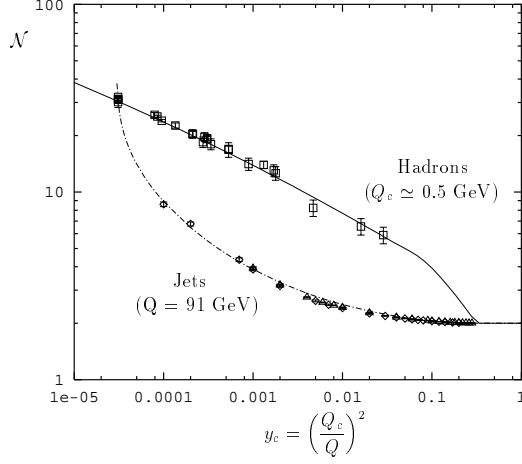


Fig. 1. Data on the average jet multiplicity \mathcal{N} at $Q = 91$ GeV for different resolution parameters y_c (lower set) and the average hadron multiplicity (assuming $\mathcal{N} = \frac{3}{2}\mathcal{N}_{ch}$) at different \sqrt{s} energies between $Q = 3$ and $Q = 91$ GeV using $Q_c = Q_0 = 0.508$ GeV in the parameter y_c (upper set). The curves follow from the evolution equation (2) with $\Lambda = 0.5$ GeV; the upper curve for hadrons is based on the duality picture (4) with $K = 1$ and parameter Q_0 (Fig. from [7])

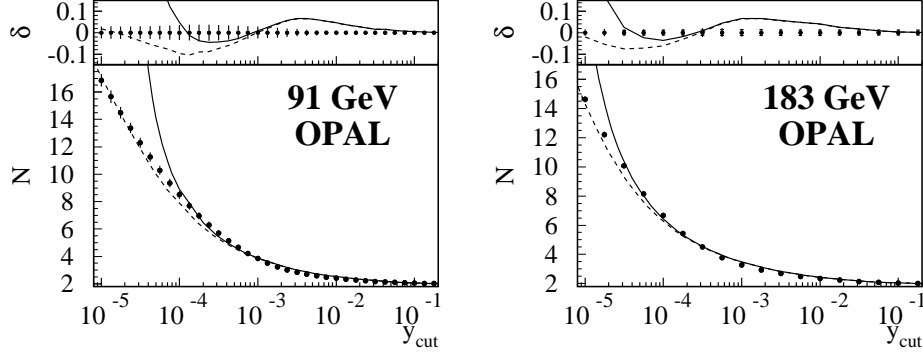


Fig. 2. Jet multiplicities extending towards lower y_{cut} parameters; full lines as in Fig. 1 for jets, dashed lines the same predictions but shifted $y_{cut} \rightarrow y_{cut} - Q_0^2/Q^2$ according to the different kinematical boundaries as in (5), with parameters as in Fig. 1 (preliminary data from OPAL [13])

multiplicity data for the cut-off parameter $Q_0 \simeq 0.5$ GeV. If this calculation is done for lower \sqrt{s} energies, agreement with all hadron multiplicity data down to $Q = 3$ GeV is obtained with the same parameter Q_0 as seen in Fig. 1 by the upper set of data and the theoretical curve. Moreover, the normalization constant in (4) can be chosen as $K = 1$ whereas in previous approximate calculations $K \approx 2$ (see, e.g. [5]). This result implies that the hadrons, in the duality picture, correspond to very narrow jets with resolution $Q_0 \simeq 0.5$ GeV.

In this unified description of hadron and jet multiplicities the running of the coupling plays a crucial role. Namely, for constant α_s both curves for hadrons and jets in Fig. 1 would coincide, as only one scale Q_{cut}/Q were available. With running $\alpha_s(k_T/\Lambda)$ the absolute scale of Q_{cut} matters: α_s varies most strongly for $Q_{cut} \rightarrow \Lambda$ for jets at small y_{cut} in the transition to hadrons and for hadrons near the threshold of the process at large y_{cut} where $\alpha_s > 1$. It appears that the final stage of hadronization in the jet evolution can be well represented by the parton cascade with the strongly rising coupling.

Preliminary results on jet multiplicities at very small y_{cut} have been obtained recently by OPAL [13] and examples are shown in Fig. 2. Whereas in the theoretical calculation all hadrons (partons in the duality picture) are resolved for $Q_{cut} \rightarrow Q_0$, for the experimental quantities this limit occurs for $Q_{cut} \rightarrow 0$.

This is an example of the kinematical mismatch between experimental and theoretical quantities discussed above and can be taken into account [7] by a shift in y_{cut} according to (5). The shifted (dashed) curves in Fig. 2 describe the data rather well (also at intermediate *cms* energies) whereby the Q_0 parameter has been taken from the fit to the hadron multiplicity before; the predictions fall a bit below the data at lower energies like 35 GeV. The nonperturbative Q_0 correction becomes negligible for $Q_c \gtrsim 1.5$ GeV.

We conclude that in case of this simple global observable the perturbative QCD calculation provides a good description of hard and soft phenomena in terms of one non-perturbative parameter $Q_0 \sim \Lambda$ (from fit [7] $Q_0 \approx 1.015\Lambda$). Multiplicity moments are described very well in this approach also [16].

4 Shape of Energy Spectrum, the Limit $\sqrt{s} \rightarrow 0$

A standard procedure in perturbative QCD is the derivation of the Q^2 evolution of the inclusive distributions – either of the structure functions in DIS ($Q^2 < 0$) or of the hadron momentum distributions (“fragmentation functions”, $Q^2 \equiv s > 0$). One starts from an input function at an initial scale Q_1^2 and predicts the change of shape with Q^2 .

In the LPHD picture one derives the parton distribution from the evolution equation (2) with initial condition (3) at threshold, here the spectrum is simply

$$D(x, Q_0) = \delta(x - 1). \quad (6)$$

If we start from this initial condition the further QCD evolution predicts the absolute shape of the particle energy distribution at any higher *cms* energy \sqrt{s} . Within certain high energy approximations one can let $Q_0 \rightarrow \Lambda$ and obtains an explicit analytical expression for the spectrum in the variable $\xi = \ln(1/x)$, the so-called “limiting spectrum” [4] which has been found to agree well with the data in the sense of (4) – disregarding the very soft region $p \lesssim Q_0$ (see, e.g. the review [2]). In the more general case $Q_0 \neq \Lambda$ the cumulant moments κ_q of the ξ distribution have been calculated as well [14,15]; they are defined by $\kappa_1 = \langle \xi \rangle = \bar{\xi}$, $\kappa_2 \equiv \sigma^2 = \langle (\xi - \bar{\xi})^2 \rangle$, $\kappa_3 = \langle (\xi - \bar{\xi})^3 \rangle$, $\kappa_4 = \langle (\xi - \bar{\xi})^4 \rangle - 3\sigma^4$,

...; also one introduces the reduced cumulants $k_q \equiv \kappa_q/\sigma^q$, in particular the skewness $s = k_3$ and the kurtosis $k = k_4$.

In the comparison with data some attention has to be paid again to the soft region. The experimental data are usually presented in terms of the momentum fraction $x_p = 2p/\sqrt{s}$, then $\xi_p \rightarrow \infty$ for $p \rightarrow 0$. On the other hand, the theoretical distribution, because of $p > p_T > Q_0$, is limited to the interval $0 < \xi < Y$, $Y = \ln(\sqrt{s}/2Q_0)$. Therefore, in this region near and beyond the boundary the two distributions cannot agree. A consistent description can be obtained if theoretical and experimental distributions are compared at the same energy as in (5), then both ξ spectra have the same upper limit Y . With a corresponding “transformation” of $E \frac{d^3n}{d^3p}$ the spectra are well described by the appropriate theoretical formula near the boundary [5].

The cumulant moments of the energy spectrum of hadrons determined in this way have been compared [5] with the theoretical calculation based on the MLLA evolution equation [15]. As seen in Fig. 3 the data agree well with the limiting spectrum result ($Q_0 = \Lambda$), both in their energy dependence and their absolute normalization at threshold (the moments vanish because of (6)). This suggests that perturbative calculations are realistic even down to threshold if a treatment of kinematic mass effects is supplemented.

Recently, results on cumulant moments have been presented by the ZEUS group at HERA (see talk by N. Brook [17]). The moments have been determined directly from the momentum distribution of particles in the Breit frame. The ξ_p distributions are seen to extend beyond the theoretical limit Y . The cumulant moments of order $q \geq 2$ determined from this distribution show large deviations from the MLLA predictions at low energies Q^2 . The kinematic effects become less important at higher energies and at $Q^2 \gtrsim 1000 \text{ GeV}^2$ the agreement with the predictions using $Q_0 = \Lambda$ is restored. These results demonstrate the importance of the soft region in the analysis of the ξ -moments.

5 Particle Spectra: the limit of small momenta p , $p_T \rightarrow 0$

In this limit simple expectations follow from the coherence of the soft gluon emission. If a soft gluon is emitted from a $q\bar{q}$ two jet system then it cannot resolve with its large wave length all individual partons but only “sees” the total charge of the primary partons $q\bar{q}$. Consequently, in the analytical treatment, the soft gluon radiation is determined by the Born term of $O(\alpha_s)$ and one expects a nearly energy independent soft particle spectrum [4]. The consequences and further predictions have been studied recently in more detail.

5.1 Energy Independence

The limit of small momenta p and p_T has been considered in [6]. The behaviour of the inclusive spectrum in rapidity and for small p_T is given by

$$\frac{dn}{dydp_T^2} \sim C_{A,F} \frac{\alpha_s(p_T)}{p_T^2} \left(1 + O \left(\ln \frac{\ln(p_T/\Lambda)}{\ln(Q_0/\Lambda)} \ln \frac{\ln(p_T/(x\Lambda))}{\ln(p_T/\Lambda)} \right) \right) \quad (7)$$

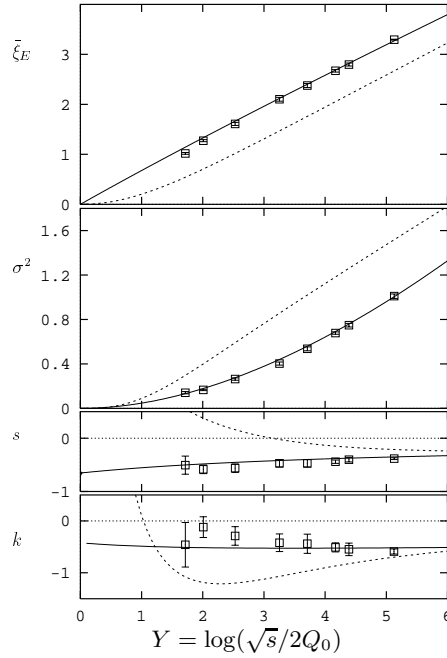


Fig. 3. The first four cumulant moments of charged particles' energy spectra i.e., the average value $\bar{\xi}_E$, the dispersion σ^2 , the skewness s and the kurtosis k , are shown as a function of *cms* energy \sqrt{s} for $Q_0 = 270$ MeV and $n_f = 3$, in comparison with MLLA predictions of the “limiting spectrum” (i.e. $Q_0 = \Lambda$) for running α_s (full line) and for fixed α_s (dashed line) (from [5])

where the second term is known within MLLA and vanishes for $p_T \rightarrow Q_0$. Again, the limit $p_T \rightarrow Q_0$ at the parton level corresponds to $p_T \rightarrow 0$ at the hadron level. Only the first term (the Born term) is energy independent. The approach to energy independence for the soft particles at $p \rightarrow 0$ is seen from e^+e^- data [5,6] and also from DIS [18], see Fig. 4. Although the detailed behaviour depends a bit on the specific implementation of the kinematic relations between partons and hadrons the approach towards energy independence in the limit $p \rightarrow 0$ is universal and this expectation is nicely supported by the data.

5.2 Colour Factors C_A and C_F

A crucial test of this interpretation is the dependence of the soft particle density on the colour of the primary partons in (7): The particle density in gluon and quark jets should approach the ratio $R(g/q) = C_A/C_F = 9/4$ in the soft limit. This factor has been originally considered for the overall event multiplicity in colour triplet and octet systems but is approached there only at asymptotically

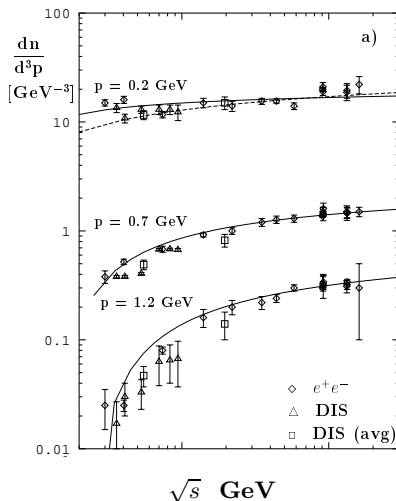


Fig. 4. Particle density at fixed momentum p as function of cms energy, from [6]

high energies [19]. On the other hand, the prediction (7) for the soft particles applies already at finite energies [6].

In practice, it is difficult to obtain gg jet systems for this test. An interesting possibility is the study of 3-jet events in e^+e^- annihilation with the gluon jet recoiling against a $q\bar{q}$ jet pair with relative opening angle of $\sim 90^\circ$ [20]. For such “inclusive gluon jets” the densities of soft particles in comparison to quark jets approach a ratio $R(g/q) \sim 1.8$ for $p \lesssim 1$ GeV which is above the overall multiplicity ratio ~ 1.5 in the quark and gluon jets but still below the ratio $C_A/C_F = 9/4$ (see Fig. 5). This difference may be attributed to the deviation of the events from exact collinearity. If the analysis is performed as function of p_T of the particles the ratio becomes consistent with $9/4$ but not for small $p_T < 1$ GeV [20]. This behaviour indicates the transition from the very soft emission which is coherent from all primary partons to the semisoft emission from the parton closest in angle (q or g) which yields directly the ratio C_A/C_F .

In order to test the role of the colour of the primary partons further in realistic processes it has been proposed [6] to study the soft particle emission perpendicular to the primary partons in 3-jet events in e^+e^- annihilation or in 2-jet production either in pp or in ep collisions, in particular in photoproduction. In these cases, for special limiting configurations of the primary partons, the particle density is either proportional to C_F or to C_A , but it is also known for all intermediate configurations. A first result of this kind of analysis has been presented by DELPHI [21] which shows the variation of the density by about 50% in good agreement with the prediction. The findings by OPAL [20] (Fig. 5) and DELPHI [21] are hints that also the soft particles indeed reflect the colour charges of the primary partons.

Important tests are possible at HERA with two-jet production from direct and resolved photons. The former process corresponds to quark exchange, the

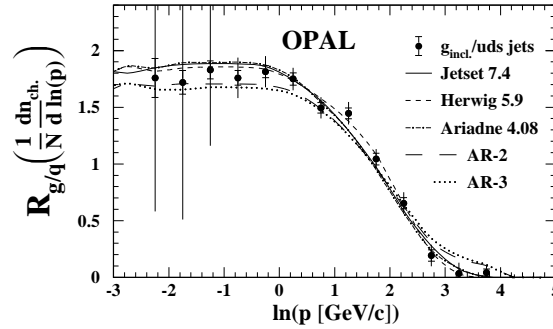


Fig. 5. Ratio of particle densities at small momenta p in inclusive gluon jets and quark jets [20]

latter to gluon exchange. The associated soft perpendicular radiation again reflects the different flow of the primary colour charges: At small scattering angles $\Theta_s \rightarrow 0$ in the di-jet cms the ratio R_\perp of the soft particles approaches the limits

$$\text{direct } \gamma p \text{ production (q exchange) : } R_\perp \rightarrow 1 \quad (8)$$

$$\text{indirect } \gamma p \text{ production (g exchange) : } R_\perp \rightarrow C_A/C_F. \quad (9)$$

In a feasibility study [22] using the event generator HERWIG these ratios have been studied as function of the particle p_T and angle Θ_s . With an assumed luminosity of 4.5 pb^{-1} significant results can be obtained. In the MC the predicted ratios are approached for small $p_T \lesssim 0.5 \text{ GeV}$ but deviate considerably for larger p_T . A study towards small angles Θ_s appears feasible. It would be clearly interesting to carry out such an analysis.

5.3 Rapidity Plateaux

Another consequence of the lowest order approximation (7) is the flat distribution in rapidity y at fixed (small) p_T . An interesting possibility appears in DIS where the soft gluon in the current hemisphere is emitted from the quark, in the target hemisphere from a gluon. This would lead one to expect a step in rapidity by factor ~ 2 between both hemispheres at high energies [6,23].

This problem has been studied recently by the H1 group [24]. They observed a considerable change of the rapidity spectrum with the p_T cut: for large $p_T > 1 \text{ GeV}$ the spectrum was peaked near $y = 0$ in the Breit frame – as expected from maximal perturbative gluon radiation – whereas for small $p_T < 0.3 \text{ GeV}$ a plateau develops in the target hemisphere. On the other hand, no plateau is observed in the current direction at all. A MC study of the e^+e^- hadronic final state did not reveal a clear sign of a flat plateau at small p_T either.

The reason for the failure seeing the flat plateau is apparently the angular recoil of the primary parton which is neglected in the result (7); this introduces

an uncertainty in the definition of p_T , especially for the higher momenta. We have investigated this hypothesis further by studying the rapidity distribution in selected MC events where all particles are limited in transverse momentum $p_T < p_T^{max}$. Then the events are more collimated and the jet axis is better defined. The MC results in Table 1 show that the rapidity density gets flatter if the transverse size of the jet decreases with the p_T^{max} cut which is in support of the above hypothesis. This selection, however, considerably reduces the event sample. A step in the rapidity hight of DIS events should therefore be expected only in events with strong collimation of particles.

Table 1. Density of particles with $p_T < 0.15$ GeV in rapidity y , normalized at $y = -1$, in events with $p_T < p_T^{max}$ selection. Results obtained from the ARIADNE MC [26] (parameters $\Lambda = 0.2$ GeV, $\ln(Q_0/\Lambda) = 0.015$ as in [25])

p_T^{max}	$y = 0$	$y = -1$	$y = -2$	$y = -3$	$y = -4$	fraction of events
no cut	1.03	1.0	0.69	0.34	0.052	100 %
0.5	0.9	1.0	0.78	0.50	0.13	9 %
0.3	0.9	1.0	0.90	0.84	0.37	0.7 %

5.4 Multiplicity Distributions of Soft Particles and Poissonian Limit

The considerations on the inclusive single particle distributions can be generalized to multiparticle distributions [25]. Interesting predictions apply for the multiplicity distributions of particles which are restricted in either the transverse momentum $p_t < p_T^{cut}$ or in spherical momentum $p < p^{cut}$.

In close similarity to QED the soft particles are independently emitted in rapidity for limited p_T : because of the soft gluon coherence the secondary emissions at small angles are suppressed. This is less so for the spherical cut. For small values of the cut parameters one finds the following limiting behaviour of the normalized factorial multiplicity moments

$$\text{cylinder : } F^{(q)}(X_\perp, Y) \simeq 1 + \frac{q(q-1)}{6} \frac{X_\perp}{Y} \quad (10)$$

$$\text{sphere : } F^{(q)}(X, Y) \simeq \text{const} \quad (11)$$

where we used the logarithmic variables $X_\perp = \ln(p_T^{cut}/Q_0)$, $X = \ln(p^{cut}/Q_0)$ and $Y = \ln(P/Q_0)$ at jet energy P . Both cuts act quite differently and for small cylindrical cut p_T^{cut} the multiplicity distribution approaches a Poisson distribution (all moments $F^{(q)} \rightarrow 1$).

This prediction is verified by the ARIADNE MC at the parton level. Interestingly, the predictions from the full hadronic final state after string hadronization yield factorial moments rising at small $p_T^{cut} < 1$ GeV. These predictions provide a novel test of soft gluon coherence in multiparticle production.

6 Conclusions and Physical Picture

The simple idea to derive hadronic multiparticle phenomena directly from the partonic final state works surprisingly well also for the soft phenomena discussed here which do not belong to the standard repertoire of perturbative QCD. Nevertheless, some clear QCD effects can be noticed in the soft phenomena and the three questions at the end of the introduction can be answered positively. A description with small cut-off $Q_0 \sim \Lambda$ is possible for various inclusive quantities. The coupling is running by more than an order of magnitude at small scales as is seen, in particular, in the transition from jets to hadrons. Also, coherence effects from soft gluons are reflected in the behaviour of soft particles. These effects for the soft particles need further comparison with quantitative predictions. Especially worthwhile are the tests on soft particle flows as function of the primary emitter configuration. Predictions exist also for nontrivial limits of multiparticle soft correlations.

The different threshold behaviour of partons and hadrons can be taken into account by appropriate relations between the respective kinematical variables. Some apparent discrepancies between MLLA predictions and observations can be related to such mass effects.

Finally, we remark on the physical picture which is supported by these results (Fig. 6). The partons in the perturbative cascade are accompanied by ultrasoft partons with $p_T \lesssim Q_0 \sim \Lambda$ as in very narrow jets; they cannot be further resolved because of confinement and therefore the perturbative partons resolved with $p_T \geq Q_0$ correspond to single final hadrons. This is consistent with the finding of normalization unity ($K = 1$ in (4)) in the transition jet \rightarrow hadron ($y_{cut} \rightarrow 0$). Colour at each perturbative vertex can be neutralized by the (non-perturbative) emission of one (or several) soft quark pairs; in this way the partons in the perturbative cascade evolve as colour neutral systems outside a volume with confinement radius $R \sim Q_0^{-1}$. In the timelike cascade there is only parton splitting, no parton recombination into massive colour singlets as in the preconfinement model. Such a picture can only serve as a rough guide, it can certainly not be complete as is exemplified by the existence of resonances. Nevertheless, its intrinsic simplicity with only one non-perturbative parameter Q_0 besides the QCD scale Λ makes it attractive as a guide into a further more detailed analysis.

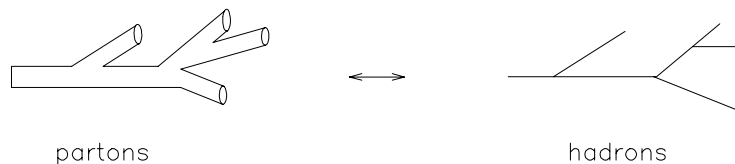


Fig. 6. Dual picture of parton and hadron cascades. Ultrasoft partons are confined to narrow tubes with $p_T < Q_0 \sim \Lambda$ around the partons in the perturbative cascade.

References

1. Yu. L. Dokshitzer, V. A. Khoze, A. H. Mueller and S. I. Troyan, *Basics of Perturbative QCD*, ed. by J. Tran Thanh Van (Editions Frontières, Gif-sur-Yvette, 1991)
2. V.A. Khoze, W. Ochs, Int. J. Mod. Phys. A **12**, 2949 (1997)
3. D. Amati, G. Veneziano, Phys. Lett. B **83**, 87 (1979)
4. Ya. I. Azimov, Yu. L. Dokshitzer, V. A. Khoze and S. I. Troyan, Z. Phys. C **27**, 65 (1985); C **31**, 213 (1986)
5. S. Lupia, W. Ochs, Phys. Lett. B **365**, 339 (1996); Eur. Phys. J. C **2**, 307 (1998)
6. V. A. Khoze, S. Lupia, W. Ochs, Phys. Lett. B **386**, 451 (1996); Eur. Phys. J. C **5**, 77 (1998)
7. S. Lupia, W. Ochs, Phys. Lett. B **418**, 214 (1998)
8. Yu. L. Dokshitzer, Proc. Durham Workshop, see W. J. Stirling, J. Phys. G **17**, 1567 (1991)
9. G. Kramer, B. Lampe, Z. Phys. C **34**, 497 (1987); C **39** (1988)
10. L3 Collaboration: O. Adriani et al., Phys. Lett. B **284**, 471 (1992)
11. OPAL Collaboration: R. Acton et al., Z. Phys. C **59**, 1 (1993)
12. S. Catani, Yu. L. Dokshitzer, M. Olsson, G. Turnock B. R. Webber, Phys. Lett. B **269**, 432 (1991)
13. P. Pfeifenschneider, thesis, Technical University Aachen, 1999; OPAL preliminary, Physics note PN403, July 1999.
14. C. P. Fong, B. R. Webber, Nucl. Phys. B **355**, 54 (1991)
15. Yu. L. Dokshitzer, V. A. Khoze, S. I. Troyan, Int. J. Mod. Phys. A **7**, 1875 (1992)
16. S. Lupia, Phys. Lett. B **439**, 150 (1998)
17. ZEUS Collaboration: J. Breitweg et al., hep-ex/9903056
18. H1 Collaboration: C. Adloff et al., Nucl. Phys. B **504**, 3 (1997)
19. S. J. Brodsky, J. F. Gunion, Phys. Rev. Lett. **37**, 402 (1976);
K. Konishi, A. Ukawa and G. Veneziano, Phys. Lett. B **78**, 243 (1978)
20. OPAL Collaboration: Abbiendi et al., hep-ex/9903027, subm. Eur. Phys. J. C.; J. W. Gary, Phys. Rev. D **49**, 4503 (1994)
21. K. Hamacher, O. Klapp, P. Langefeld, M. Siebel, DELPHI 99-115 CONF 302, subm. to the HEP'99 Conference, Tampere, Finland, July 1999
22. J. M. Butterworth, V. A. Khoze and W. Ochs, J. Phys. G **25**, 1457 (1999)
23. W. Ochs, in *Proc. Ringberg Workshop 'New Trends in HERA Physics', Tegernsee, Germany 1997*, ed. by B. A. Kniehl, G. Kramer, A. Wagner (World Scientific, Singapore, 1998) p. 173
24. H1 Collaboration: C. Adloff et al. in: *29th Int. Conf. on High Energy Physics, Vancouver, Canada, July 1998*, paper 531; K. T. Donovan, D. Kant, G. Thompson, J. Phys. G **25**, 1448 (1999)
25. S. Lupia, W. Ochs, J. Wosiek, Nucl. Phys. B **540**, 405 (1999)
26. L. Lönnblad, Comp. Phys. Comm. **71**, 15 (1998)